A Novel Approach to Fingerprint Pore Extraction

Michael Ray, Peter Meenen, and Reza Adhami
Department of Electrical and Computer Engineering
The University of Alabama in Huntsville
Huntsville, AL 35899 USA
pmeenen@ece.uah.edu

Key Words: Image Processing, Biometrics, Fingerprints, Pores

Abstract -- Automated Fingerprint Identification Systems (AFIS) have become a popular tool in many security and law enforcement applications. Most of these systems rely on the matching of fingerprints using the position and orientation of ridge endings and bifurcations within the fingerprint image. While this information is sufficient for matching fingerprints in small databases, it is not discriminatory enough to provide good results on large collections of fingerprint images. This paper presents a means of obtaining additional discriminatory information from fingerprint images by demonstrating a novel method to extract the locations of sweat pores from the grayscale fingerprint image. This is achieved through the implementation of a modified minimum squared error approach. The proposed algorithm is capable of obtaining good results even from images obtained from basic 500 dpi optical live-scan devices despite the common belief that images obtained at this resolution are not of high enough quality. Results of the proposed method are demonstrated on fingerprint images taken both from a common live-scan device and the inked prints of the NIST 4 database. An explanation of the approach is presented, the results are discussed, and future research possibilities are put forth.

I. INTRODUCTION

With the current international focus on improved security, the idea of using physical and psychological traits of an individual, also known as biometrics, for positive identification has become increasingly popular [1],[2]. Of the biometrics currently implemented in automated personnel identification systems (APID), the fingerprint is one of the most popular. This is primarily because of the ease of collection and highly unique structure of the fingerprint. A given fingerprint consists of a series of alternating ridges and valleys that cover the surface of the finger. These ridges form a unique pattern as they flow across the surface of the finger. The local and global characteristics of these ridges can therefore be used to uniquely identify an individual [3].

Ridge characteristics are typically divided into three classes or levels based upon the discriminatory ability of the feature. Level one detail consists primarily of the global pattern class formed by the ridge structure, for example a loop or a whorl pattern. Level two detail encompasses the position and orientation of the ridge endings and bifurcations along with the paths taken by individual ridges, and level three detail consists of extremely fine detail, such as the location of sweat pores [4].

Most of the current automated fingerprint identification systems utilize discriminatory information taken only from the first and second levels of detail. In fact, most systems only use the pattern class from level one coupled with the position and orientation of the ridge endings and bifurcations from level two. Unfortunately, this means that a large amount of fingerprint detail is ignored [5]. The detail available in level three is seldom if ever used due to the difficulty that is typically associated with the extraction of this information. While this may have been the case with many of the older live-scan devices, the current devices are capable of detecting a reasonable amount of level three detail even at the relatively limited 500 dpi resolution. The most promising information that can be extracted from the third level of detail is the location of the sweat pores along the ridges. An example of pores in a fingerprint image is given in Figure 1.

Previous attempts to extract pore detail relied on very high resolution images and extracted the pore locations by processing the skeleton of the fingerprint image [6],[7]. While this is a valid approach to pore extraction, it is very impractical because it requires considerable computational power and expensive

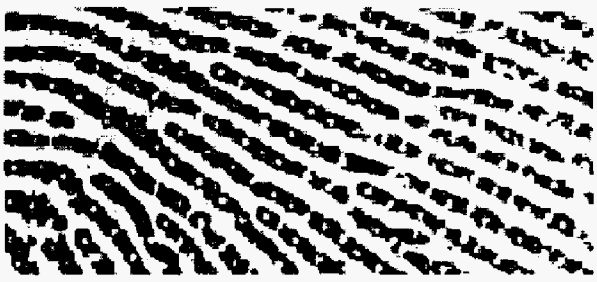

Figure 1. An example of pores (white dots) on the ridges within a fingerprint image.

0-7803-8808-9/05/$20.00 ©2005 IEEE

scanning devices to implement. In this paper, we propose a novel approach to the detection of pores from within the grayscale image. Not only does this mean that the image does not need to be processed down to a skeleton, but it also allows for the extraction of the pore locations from lower resolution images, including many of the standard 500 dpi images obtained by present-day live-scan devices.

The remainder of this paper is divided into three sections. In section II, the new method for pore extraction will be presented. This method utilizes a minimum squared error technique combined with several other operations to isolate the positions of the pores along the ridges of the fingerprint. In many cases, pores are not extractable on all of the ridges, particularly when dealing with low quality, very dry, or low resolution images. The proposed algorithm does a good job of locating the remaining visible pores and it can do so with a high level of reproducibility. In section III the results of applying the proposed algorithm to various fingerprint images, including those from both live-scan devices and the NIST 4 database will be given. Finally, in section IV the conclusions and some suggestions for future research will be set forth.

II. PORE EXTRACTION

Before describing the pore extraction method, it is necessary to know what a typical pore looks like. This information is essential so that the extraction algorithm will know what to look for. As a result, a large number of pores were manually extracted from fingerprint images and examined in order to construct a model that could be used in the extraction stage. As it turned out, the majority of pores within a 500 dpi image can be approximated using a slightly modified 2-dimensional Gaussian function as follows:

$$M(x,y) = 1 - e^{-\left|x^2+y^2\right|^{\frac{1}{2}}} \qquad (1)$$

The size of the model used is also important, since larger models greatly increase the computing resources required in the extraction stage. These larger models may be necessary, however, to extract the larger pore structures evident at higher resolutions. It was found that for a typical 500 dpi image, the majority of pores could be quickly and reliably located using a 3 x 3 model. A plot of the fingerprint pore model and the resulting 3 x 3 filter are shown in Figure 2.

Now that the pore extraction algorithm has a model for an average pore, it knows what to look for in the fingerprint image, and can be applied to extract the

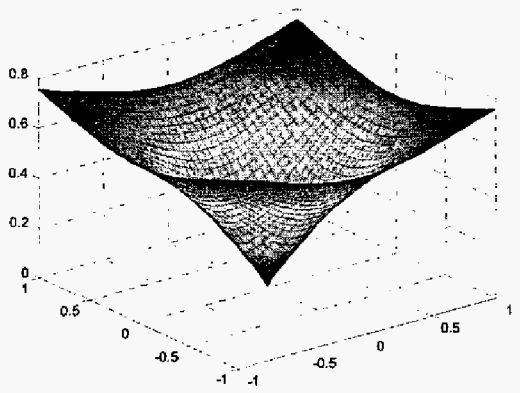

0.7569	0.6321	0.7569
0.6321	0	0.6321
0.7569	0.6321	0.7569

Figure 2. A high resolution example of the pore model and the 3 x 3 pore mask obtained by sampling it.

locations of the pores. This process begins by preparing the input fingerprint image for processing. This particular method requires a fingerprint image in which the ridges are represented in white and the valleys are in black. This is the negative of the fingerprint images produced by most fingerprint scanners. Thus, the first step in the process is to negate the original grayscale image. The new negative image values, *N(x, y)* can be found by simply applying the following basic negation equation:

$$N(x,y) = 255 - I(x,y). \qquad (2)$$

Next, the image must be normalized so that the pixel intensities of the resulting image, *F(x, y)*, will fall within a range from 0 to 1, where 1 represents pure white and 0 represents pure black. Once again this is performed by using a basic image normalization equation as follows:

$$F(x,y) = \frac{N(x,y)}{255}. \qquad (3)$$

With the input image prepared, the location of the pores can begin. This process begins by centering the

pore model above each pixel in the normalized and inverted fingerprint image and calculating the sum of the squared error for that 3 x 3 overlap. In other words, for each pixel *F(x, y)* in the fingerprint image the resulting sum of the error, *E(x, y)*, is calculated as follows:

$$E(x,y) = \sum_{i=x-r}^{x+r} \sum_{j=y-r}^{y+r} \left[F(i,j) - M(i-x+r, j-y+r)\right]^2 \quad (4)$$

where M is the pore model and r is the distance from the center of the model to the edge. In the case of a 3 x 3 pore model for example, a value of $r = 1$ would be used.

The error map found in Equation 4 reveals the areas within the image that have a high probability of containing pores. To make the error map more helpful, it is processed by a thresholding operation in order to provide a binary image in which areas of high pore probability (low error) are represented as white (1) and areas of low pore probability (high error) are represented as black (0). The binary image that results from this process is labeled $E_B(x, y)$. An example of a typical binarized error map can be found in Figure 3.

Now that the areas likely to contain pores have been identified, the next step is to find the precise locations of the pores within these areas. The first step in this process is to locate the points in the original error map, *E(x, y)* that possess the minimum amount of local error.

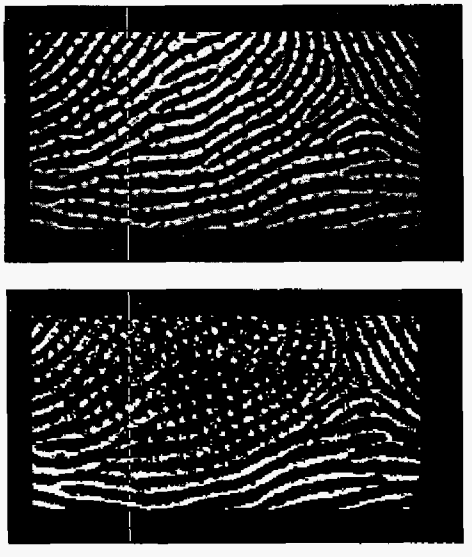

Figure 3. An example of part of a fingerprint image (top) and the binarized error map that is generated from it (bottom).

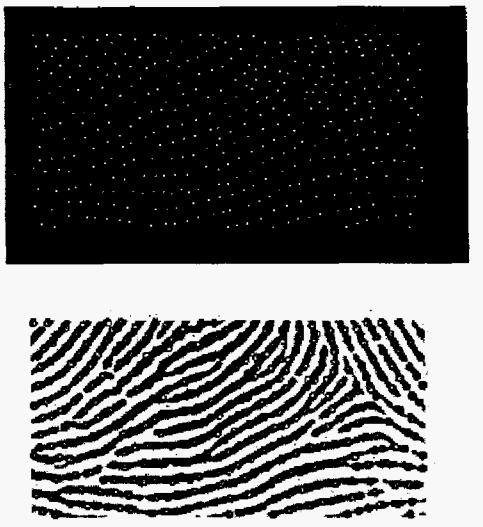

Figure 4. An example of the pores extracted from the fingerprint image shown in Figure 3 (top) and an overlay of the detected pores and the fingerprint image (bottom).

In other words, the points which possess the lowest error within a local neighborhood, typically 5 x 5 or 7 x 7 are located and stored as a binary image using the following equation:

$$M_L(x,y) = \begin{Bmatrix} 1 \text{ if } E(x,y) = \min[B_L] \\ 0 \text{ otherwise} \end{Bmatrix} \quad (5)$$

where B_L is the local neighborhood around the point (x,y). This neighborhood can be defined as:

$$B_L = E(x - r_m : x + r_m, y - r_m : y + r_m) \quad (6)$$

where r_m is the distance from the center point of the neighborhood to its edge. The points of minimum local error found by Equation 5 are then filtered by the binarized error map. This step is necessary to remove any points of minimum local error that are not within a probable pore area. This is achieved by a simple point-by-point multiplication between the binary image containing the local minima points and the binarized error map. Thus, the positions of the final pore locations, *P(x, y)*, can be found by using :

$$P(x,y) = E_B(x,y) M_L(x,y). \quad (7)$$

Thus, the locations of the pores within the image have been found. An example of the results of this process can be seen in Figure 4.

It should be noted that in some instances, particularly in lower quality fingerprint images that contain a fair amount of noise, some spurious pore locations may be found in the valleys of the fingerprint image. To prevent this from occurring, an optional final step can be performed in which the results of the pore location process are masked by the fingerprint image binarization. This insures that pores can only be found on the ridges of the fingerprint. This step is seldom necessary in high quality fingerprint images, however.

III. RESULTS

The results of employing the pore extraction method outlined in Section 2 are very promising. The visual results of applying the algorithm to an image obtained by a common optical scanner have already been seen in Figure 4. The method also performs surprisingly well on inked fingerprint images, such as those in the NIST database. With inked fingerprints, there is more noise and as a result, more spurious pore locations. Figure 5 demonstrates the results of applying the extraction algorithm to an image taken from the NIST 4 database.

Aside from the basic visual results, the algorithm output was tested in two ways, first for accuracy, and secondly for reproducibility. The output was tested for accuracy by manually noting the locations of visible pores within a set of 10 fingerprint images. All of these images were then processed by the pore extraction algorithm and the pores locations that it determined were compared to the manually determined locations. In this test, the method achieved better than 90% accuracy, with the two most common problems being the missing of pores at the very edge of ridges and occasionally missing pores that were unusually large. The reproducibility of the algorithm was tested by applying it to several impressions of the same finger and using an automated point matching system to determine the similarity of the overlapping regions of the impressions. The similarity score was calculated by dividing the number of matching pores to the total number of pores in the overlapping regions. In these tests, multiple impressions of 20 different fingerprints were compared and the typical similarity scores were around 85%. These scores are fairly good considering the high impact of elastic distortion on pore locations. Figure 6 shows an overlay of the pores extracted from two impressions of the same finger. The larger circle in this overlay indicates the two pores on which the overlay was aligned.

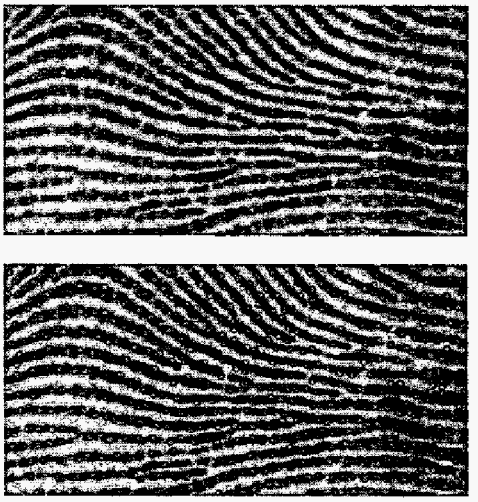

Figure 5. An example of the results obtained when applying the pore extraction algorithm to a NIST image

IV. CONCLUSIONS

In this document, a novel method for the extraction of pore information from fingerprint images has been proposed. The steps involved in the extraction process have been outlined and some example results have been

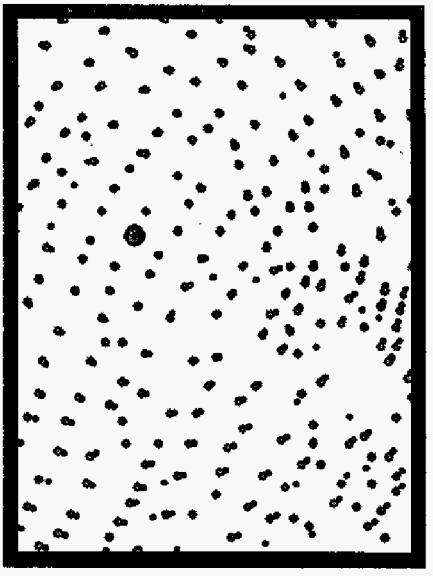

Figure 6. An example of the reproducibility of the pore extraction method. Here the pores extracted from one instance of a fingerprint (small black dots) are overlaid on top of the pores extracted from a second instance of the same finger (larger gray dots). The largest dot indicates the two pores used for alignment.

shown for both live-scan and inked fingerprint images. The results show that this method holds promise for the reproducible location and use of pore information by fingerprint identification systems. While not every fingerprint image obtained with a 500 dpi scanner has evident pores, a substantial number of them do. As a result, it is a natural step to try to extract this information to aid in the matching process. In addition, the ever increasing quality of the images obtained from sensors and the higher resolutions that new sensors will be capable of requires that the pore information in fingerprints be considered. This means that there will be a considerable amount of future research potential in the areas of improved methods for extracting pores and new and better ways of incorporating the pore information into the fingerprint matching system. The method proposed in this document represents only one of the first approaches to the pore extraction problem and will lead to new and improved matching systems in the future.

V. BIBLIOGRAPHY

[1] A.K. Jain, R. Bolle, and S. Pankanti, eds., *Biometrics: Personal Identification in a Networked Society,* Kluwer Academic Publishers, 1999.

[2] P. Meenen and R. Adhami, "Fingerprinting for Security," *IEEE Potentials*, vol. 20 no. 3 Aug./Sept. 2001, pp. 33 – 38.

[3] Harold Cummins and Charles Midlo, *Finger Prints, Palms and Soles: An Introduction to Dermatoglyphics,* South Berlin, MA: Research Publishing Company, 1976.

[4] David R. Ashbaugh, *Quantitative-Qualitative Friction Ridge Analysis: An Introduction to Basic and Advanced Ridgeology,* New York: CRC Press, 1999.

[5] S. Pankanti, S. Prabhakar, and A.K. Jain, "On the Individuality of Fingerprints," *IEEE Transactions on Pattern Analysis and Machine Intelligence*, vol. 24, no. 8, Aug. 2002, pp. 1010 – 1025.

[6] J. D. Stosz, and L. A. Alyea, , "Automated System for Fingerprint Authentication Using Pores and Ridge Structure," *Proc. SPIE, Automatic Systems for the Identification and Inspection of Humans, San Diego, CA*, Vol. 2277,, pp. 210-223, July 1994.

[7] A.R. Roddy and J. D. Stosz, "Fingerprint Features-Statistical Analysis and System Performance Estimates," *Proceedings of the IEEE*, vol. 85, no. 9, pp. 1390 –1421, Sept. 1997.